International Journal of Science and Research (IJSR)
ISSN (Online): 2319-7064
Index Copernicus Value (2015): 78.96 | Impact Factor (2015): 6.391

Broadband Photocurrent Enhancement in Longwave Infrared Quantum Dot Photodetectors by Sub-Wavelength Surface Gratings

Arpana Mishra

Abdul Kalam Technical University, G. L. Bajaj Institute of Technology and Management, Greater Noida, U.P.-201306, India

Abstract: ***Broadband photocurrent enhancement covering the wavelength range from 4 µm to 11 µm is observed. A 4.6 times (4.6x) photocurrent enhancement is obtained at the photodetection wavelength of 8.7 µ m. By comparing the simulated diffraction efficiency with the photocurrent enhancement spectrum, we attribute the enhancement to the 1st-order diffraction of the normal infrared (IR) incidence radiation. The photodetectivity (D*) enhancement at different biases is also measured and analyzed.***

Keywords: Quantum dot infrared photodetector (QDIP); sub-wavelength surface gratings; broadband photocurrent enhancement

1. Introduction

Quantum dot infrared photodetectors (QDIPs) and focal plane array (FPA) based on intersubband transitions in self-assembled quantum dots (QD) show promising potential for middle wave (3 to5 µm) infrared (MWIR) and long wave (8 to12 µm) infrared (LWIR) sensing and imaging.The three-dimensional (3D) quantum onfinement structure provides several advantages, including normal incidence photodetection, lower dark current, high photoreponsitivities , and high operating temperature. However, since the number of active QD layers is limited by the strain and the strain induced defects and dislocations, QDIPs show low quantum efficiencies (QE). Various enhancement techniques have beendeveloped to improve the performance of QDIPs, including: (1) reflection surface grating structures (RSG); (2) photonic crystal (PC) cavity enhanced QDIP; and (3) surface plasmonic resonance (SPR) enhanced QDIPs.The PC cavity and the SPR enhancement are Optics and based on resonant effects and are therefore unable to achieve broadband enhancement. In this paper, we report a broadband QDIP enhancement technology based on sub-wavelength transmission surface gratings (TSG). Photocurrent enhancement of 2 to 4.6 times is obtained at a broadband wavelength range from 4 to 11 µm. By comparing the simulated diffraction efficiency with the photocurrent enhancement spectrum, we attribute the photocurrent enhancement to the 1st-order diffraction induced coupling of the normal infrared (IR) incidence radiation (x- or y-polarization) to the z-polarized IR incidence. The photodetectivity (D*) enhancement at different biases is also measured and shows smaller photodetectivity enhancement at higher negative bias levels, suggesting that the high negative bias favors the photocurrent generation with the normal IR incidence.

2. Device Fabrication

The QD sample is grown by using a Veeco Gen II MBE system via the Stranski-Krastanow (SK) growth mode. A 0.3 µ m Si-doped (n+) GaAs bottom contact layer (n = 1 x10^{18} cm^{-3}) is first grown on a semi-insulating GaAs (100) wafer, followed by the growth of a 100 nm undoped GaAs buffer layer. The growth temperature for the GaAs contact and buffer layers is set to 580 ^{o}C. The QD absorption region is then grown. The QDIP absorption region consists of ten-period stacked QD layers. Each QD layer consists of 2.4 monolayer (ML) of InAs QD and 20ML of InGaAs as capping layers. The QD regions are separated by 65nm GaAs spacer layers. The n-doping level of the QD region is estimated to be 3.5x10^{17} cm^{-3}, corresponding to 2 electrons doping per QD. The QD layers and cap layers are grown at ~ 480 ^{o}C. The QD active layer is then covered by a 20 nm undoped Al0.20Ga0.80As top current-blocking layer and 0.1 µ m highly Si-doped (n = 1 x10^{18} cm^{-3} , GaAs contact layers. A 1.8 µ m-thick undoped GaAs layer is finally grown on top of the top n+ GaAs contacting layer.

After the growth, the wafer is processed into 250 µ m-diameter circular mesas using standard photo-lithography and wet etching procedures. The sub-wavelength surface grating structure is then fabricated on top of the QDIP mesa by using the reactive ion etching (RIE) process. The depth of the sub-wavelength surface gratings is 1.8 µ m.

Finally, the top and bottom electrodes are formed by using the E-beam metal evaporation deposition, lift-off and thermal annealing processes. The top and bottom electrodes were conventional N-type Ni/AuGe/Au (150 A^{0}/300A^{0}/4000A^{0}) alloys. We have verified that the deposited Ni/AuGe/Au layer can effectively cover the top gratings and provide an Ohmic contact to the top contacting layer of the QDIP.

The top view and the zoom-in view of the QDIP with the top sub-wavelength TSG structures are shown in Figs. (1a) and 1(b), respectively. The sub-wavelength TSG structure is a square lattice with a lattice constant a= 4.2 µ m. The width of the square is d = 2.1 µ m.

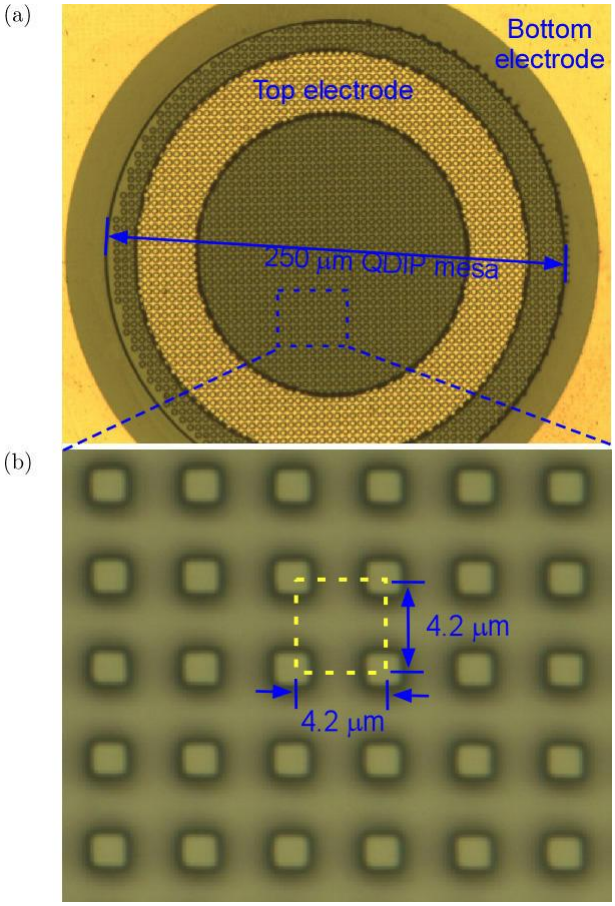

3. Results and Discussions

Figure 2 shows the photocurrent spectrum of the QDIP-TSG4.2 (upper trace) and the Ref- QDIP (lower trace) at sample emperature of 77K at the bias voltage of -1.0 V. The QDIPTSG4.2 sample shows a broadband 2 to 4.6 times photocurrent enhancement from 4 μm to 11 μm. At the wavelength of 8.7 μm, a 4.6 times photocurrent enhancement is obtained. The insets show the configurations of the TSG structure used in the simulation. At long wavelengths from 5-11μm, the 1st-order transmission diffraction efficiency shows a similar trend to the photocurrent enhancement of the QDIP-TSG4.2 sample .The photocurrent enhancement at these wavelengths is primarily due to 1st-order diffraction which couples the normal infrared (IR) incidence radiation (x- or y-polarization) to the z-polarized IR incidence. The enhancement at shorter wavelength ranges from 3.5 to 5μm can be therefore attributed to higher order diffraction.

4. Conclusion

In conclusion, a long wave infrared quantum dot photodetector with the top subwavelength TSG structure is fabricated. A 2 to 4.6 times broadband photocurrent enhancement is obtained at a broadband wavelength range from 4 to11μm. The sub-wavelength surface grating structures are simulated and the photocurrent enhancement at long wavelengths from 5 to11 μm is attributed to the 1st-order diffraction induced coupling of the normal infrared (IR) incidence radiation (x- or y-polarization) to the z-polarized IR incidence. The photodetectivity (D*) enhancement at different biases is also measured and the smaller photodetectivity enhancement at higher negative bias levels suggests that the high negative bias favors photocurrent generation with the normal IR incidence.

References

[1] E. Ip, et al., JLT, vol.26, pp.3416-3425, 2008. [7] W. Shieh, et al., IEEE Photonics J., vol.2, pp. 276-283.
[2] L. Du, et al., OE, vol.19, pp.8079-8084, 2011. [12] Q. Zhuge, et al., OE, vol.20, pp.19599-19609, 2012
[3] P. Bhattacharya, X. H. Su, S. Chakrabarti, G. Ariyawansa and A. G. U. Perera, Characteristics of a tunneling quantum-dot infrared photodetector operating at room temperature, Appl. Phys. Lett. 86 (2005) 191106
[4] L. Jiang, S. S. Li, N. Yeh and J. Chyi, In0:6Ga0:4As/GaAs quantum-dot infrared Photodetector with operating temperature up to 260 K, Appl. Phys. Lett. 82 (2003) 1986_1988
[5] Operating temperature 320 _ 256 middlewavelength infrared focal plane array imaging based on an InAs/InGaAs/InAlAs/InP quantum dot infrared photodetector, Appl. Phys Lett. 90(20) (2007) 201109
[6] S. Krishna, S. D. Gunapala, S. V. Bandara, C. Hill and D. Z. Ting, Quantum dot based infrared focal plane arrays, Proceed. of the IEEE 95(9) (2007) 1757_1766.
[7] S. Gunapala, S. Bandara, C. Hill, D. Ting, J. Liu, Sir B. Rafol, E. Blazejewski, J. Mumolo, S. Keo, S. Krishna, Y. Chang and C. Shott,